Published in Contributions to Mineralogy and Petrology 121, issue 1, 45-60, 1995
which should be used for any reference to this work

Angelika Kalt · Rainer Altherr · Michael Hanel

Contrasting P-T conditions recorded in ultramafic high-pressure rocks from the Variscan Schwarzwald (F.R.G.)

Abstract This paper presents mineralogical and textural data as well as thermobarometric calculations on ultramafic high-pressure rocks from the Variscan basement of the Schwarzwald (F.R.G.). The rocks form small isolated bodies within low-pressure / high-temperature gneisses and migmatites. The results of this study constrain contrasting *P-T* evolutions for four garnet-bearing ultramafic high-pressure rocks. Two magnesian garnet-spinal peridotites sampled near the southern margin of the Central Schwarzwald Gneiss Complex (CSGC) were equilibrated at 670–740° C and 1.4–1.8 GPa. These *P-T* conditions are similar to those recorded by eclogites intercalated in the same basement unit. Two garnet websterites sampled from the northern part of the CSGC have comparatively low Mg/(Mg + Fe) and low Cr and Ni abundances and are interpreted as former cumulates. These rocks most probably experienced an initial high-temperature stage within the spinel peridotite stability field, followed by re-equilibration at 740–850° C / 3.2–4.3 GPa and subsequent recrystallization at lower pressures. Further petrologic studies have to reveal whether ultramafic high-pressure rocks of the Schwarzwald can generally be assigned to these two groups which are mainly defined by contrasting peak pressures.

Introduction

High-pressure (H*P*) rocks of mantle or crustal origin are the most crucial pieces of evidence for reconstructing orogenic processes in collisional belts. In particular, ultramafic garnet-bearing peridotites and pyroxenites have frequently been used to monitor subduction and collision processes within various orogens.

Depending on the evolution of garnet-bearing ultramafic H*P* rocks, different aspects of orogenic processes can be constrained. The rocks may represent garnetiferous upper mantle emplaced into the continental crust (Medaris et al. 1990), giving evidence of crustal stacking and thickening. Garnet-bearing ultramafic rocks can also be derived from high-temperature (H*T*) spinel-bearing lithologies that crystallized at (near-) solidus temperatures and subsequently passed into the garnet peridotite or garnet pyroxenite stability field by cooling (Medaris and Carswell 1990 and references cited therein), thus indicating a melting event within the upper mantle. Garnet-bearing ultramafic rocks may also be generated by prograde H*P* metamorphism of either spinel peridotites and serpentinites that had previously been emplaced into the crust as parts of ophiolite complexes (Ernst 1978; Evans and Trommsdorff 1978; Obata 1980) or low-pressure (L*P*) cumulate rocks belonging to layered intrusions (Jamtveit 1987a, b). In these cases subduction of oceanic crust or burial of continental crust is monitored.

Distinction between the different possible origins for ultramafic H*P* rocks is a prerequisite for unravelling the complex tectonometamorphic histories of collision belts. One promising approach is the establishment of *P–T* paths or *P–T–t* paths on the basis of mineralogical and textural data as well as by geothermobarometric calculations and isotope dating. Especially for the Variscan belt, petrological and geochronological studies on peridotites (Bonnot and Piboule 1980; Carswell and Jamtveit 1990; Medaris et al. 1990; Brueckner et al. 1991; Beard et al. 1992) have revealed rather diverse *P–T* (*-t*) paths for these rocks and have thus led to the recognition of distinct tectonometamorphic units within the Variscan orogen.

A. Kalt (✉) · R. Altherr · M. Hanel
Mineralogisch-Petrographisches Institut, Universität Heidelberg, Im Neuenheimer Feld 236 D-69120 Heidelberg, Germany

M. Hanel
Mineralogisch-Petrographisches Institut, Universität Freiburg, Albertstrasse 23b, D-79104 Freiburg, Germany
Editorial responsibility: J. Hoefs

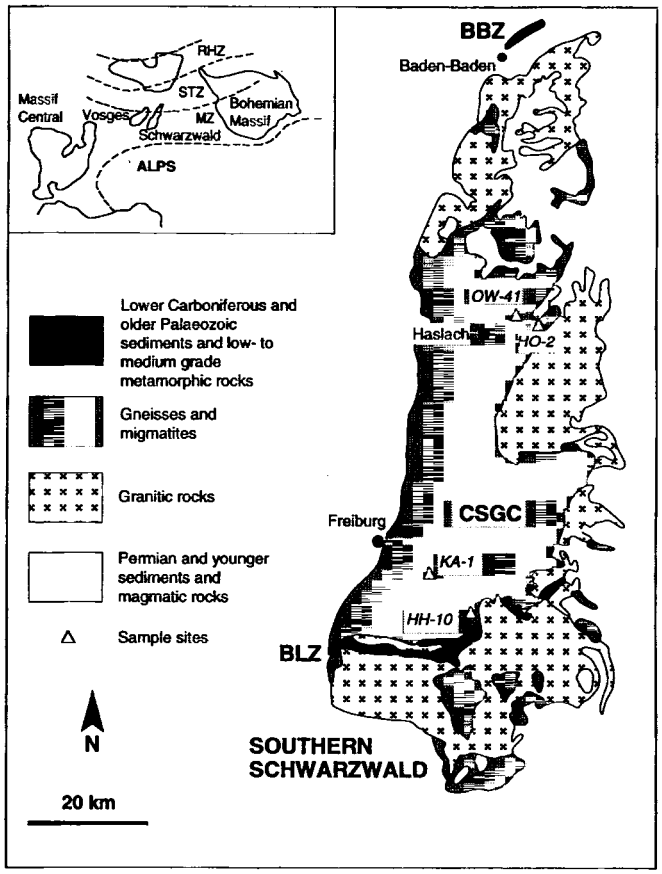

Fig. 1 Map of the Schwarzwald showing sample localities and geological features mentioned in the text

The purpose of the current investigation is to present mineralogical and petrological data on garnet peridotites and pyroxenites from the Variscan Schwarzwald that have not been documented before. The conditions of equilibration and the P–T evolution of these ultramafic HP rocks must carefully be set out in order to place constraints on the tectonometamorphic evolution of the Schwarzwald as a part of the Moldanubian zone of the Variscan belt.

Geological setting and sample locations

The Schwarzwald is part of the central Variscan belt (Fig. 1). It comprises two units of low to medium-grade metamorphic Paleozoic sediments and volcanic rocks, the Baden-Baden Zone (BBZ) to the north and the Badenweiler-Lenzkirch Zone (BLZ) to the south. During Variscan convergence a Moldanubian high-grade metamorphic basement nappe, the Central Schwarzwald Gneiss Complex (CSGC), was tectonically emplaced over those units (Eisbacher et al. 1989; Wickert et al. 1990). To the south, the BLZ is bordered by a second high-grade metamorphic unit, the Southern Schwarzwald (Fig. 1) which is also assigned to the Moldanubian Zone.

The CSGC and the Southern Schwarzwald mainly consist of metapsammitic gneisses and migmatites that experienced the peak of high-temperature (HT) metamorphism at 335–330 Ma B.P. (Kalt et al. 1994a). Apart from this rather monotonous series, the CSGC also contains more variegated gneiss lithologies and metagranitic rocks. Nevertheless, an internal nappe pile character as for example inferred for the corresponding Moldanubian basement of the Vosges (Rey et al. 1991) from P–T estimations and structural observations has not yet been established for the CSGC.

Both the CSGC and the Southern Schwarzwald are intruded by granite plutons dated at 335–310 Ma B.P. (Wendt et al. 1974; Todt 1976, compilation in Echtler and Chauvet 1991/92) and bear intercalations of granulites as well as isolated bodies of ultramafic HP rock or relics of those. Most of the ultramafic rocks have been subject to intensive retrogression and weathering. While serpentinites and spinel peridotites are present in both units, garnet-bearing ultramafic HP rocks and eclogites have only been found within the gneisses and migmatites of the CSGC so far. High-pressure metamorphism for four representative eclogite samples equilibrated at temperatures of 670–750° C and minimum pressures of about 1.6 GPa was dated at 337–332 Ma B.P. (Kalt et al. 1994b).

Sample locations of garnet-bearing ultramafic rocks described in this paper are indicated in Fig. 1 and described in the appendix. Two sampling sites (HH-10 and KA-1) are located near the southern margin of the CSGC while the other two (OW-41 and HO-2) lie within the northern part of the CSGC. Two of the four samples were found as single block (HO-2) and as accumulation of several blocks (HH-10; first described by Wimmenauer and Schreiner 1981). Samples OW-41 and KA-1 were collected from metre-sized lens-shaped bodies included in migmatic gneisses. Unfortunately, no contacts with the host rocks are exposed.

Textures, mineral compositions, and evolutionary stages

The four investigated samples form two distinct groups in terms of bulk rock chemistry, phase compositions, and textures. Compared to average garnet peridotites, the garnet websterite samples HO-2 and OW-41 are ferriferous with Mg/(Mg + Fe) = (X_{Mg}) of 0.675 for HO-2 and of 0.610 for OW-41, poor in Cr (1000 and 1300 ppm, respectively) and Ni (85 and 110 ppm, respectively), and contain Fe and Ti oxide phases. The rocks comprise relatively Fe-rich pyroxenes, garnet, and olivine (only OW-41) and partly show porphyroclastic textures. Although their TiO_2 contents are not conspicuously high (0.38 and 0.67 wt%), samples HO-2 and OW-41 correspond to the Fe–Ti garnet peridotite type defined for the Western Gneiss Region in Norway (Carswell et al. 1983; Medaris and Carswell 1990).

On the contrary, samples HH-10 and KA-1 are magnesian garnet-spinel peridotites with Mg-rich olivine, pyroxenes and garnet that are comparable to the Mg-Cr garnet peridotite type defined by Carswell et al. (1983) and Medaris and Carswell (1990) in terms of composition. Both samples contain primary Cr-Al spinel and pargasitic amphibole and are foliated.

Garnet-olivine websterite OW-41

The rock is fine grained and mainly composed of garnet, orthopyroxene, clinopyroxene, and olivine. Minor phases are Ca-amphibole, serpentine, spinel, rutile, magnetite, and ilmenite. Textures and mineral compositions reflect a polymetamorphic evolution.

A porphyroclastic relic texture is formed by large orthopyroxene porphyroclasts and rare medium-sized clinopyroxene porphyroclasts, bordered by olivine grains which have been strongly retrogressed to serpentine and magnetite (Fig. 2a). Between the pyroxene porphyroclasts and olivine, medium-sized garnet clusters as well as a granoblastic matrix of smaller clinopyroxene, orthopyroxene and garnet grains have developed. Amphibole may in places coexist with the granoblastic matrix but mainly overgrows it.

Olivine grains contain rare inclusions of Cr-Al spinel. Clinopyroxene porphyroclasts have many tiny inclusions of ilmenite

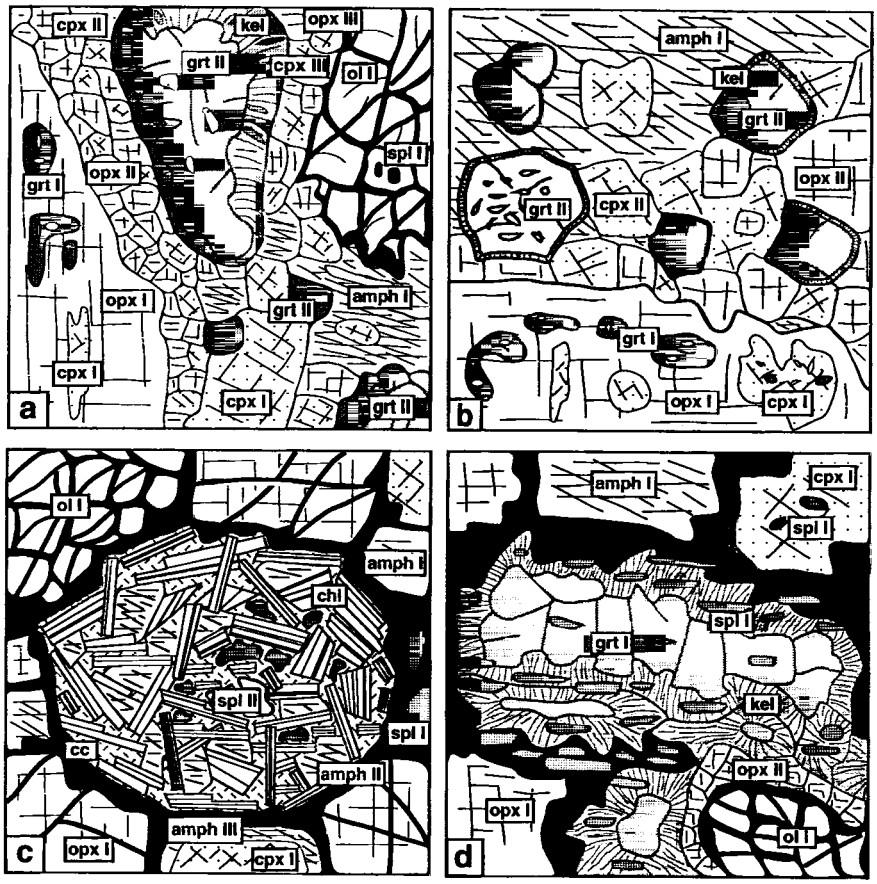

Fig. 2a–d Schematic representation of some important textural features. For mineral abbreviations and detailed descriptions see section on textures, mineral compositions, and evolutionary stages in the text. *Black areas* represent secondary serpentine. **a** Garnet-olivine websterite OW-41: marginal part of a large opx I porphyroclast with inclusions of grt I (with inclusions of opx I and cpx I) and cpx I and a recrystallized rim consisting of opx II, cpx II, grt II, and amph I. Ol I contains inclusions of primary Cr-Al spinel (spl I). **b** Garnet websterite HO-2: Opx I porphyroclast (*lower part*) containing cpx I, and grt I, and recrystallized domain (*upper part*) with polygonal grains of grt II, cpx II, opx II, and poikiloblastic amph I. **c** Garnet–spinel peridotite HH-10: round aggregate consisting of chlorite, tremolite (*amph II*), Cr-Al spinel (*spl II*), and calcite (*cc*), interpreted as pseudomorph after garnet in a serpentinized matrix of ol I, opx I, cpx I, and spl I. **d** Garnet-spinel peridotite KA-1: elongate porphyroblasts of grt I with included trails of spl I and an inclusion of partly serpentinized ol I. At the contact with kelyphite (*amph II, Cr-poor spl II*), olivine is rimmed by a corona of opx II

and rutile, a few garnet inclusions and very rare relics of Cr–Al spinel. Orthopyroxene porphyroclasts show inclusions of garnet, clinopyroxene and, more rarely, of olivine and rutile. The garnet inclusions in turn contain tiny orthopyroxene and clinopyroxene grains. The fact that garnet forms inclusions in pyroxenes and bears the latter as inclusions itself along with the elongate shape and sub-linear arrangement of some garnet and clinopyroxene inclusions in orthopyroxene suggests that, although modified by later recrystallization, garnet and the large clinopyroxene and orthopyroxene porphyroclasts were originally derived by unmixing from former *HT* Al-rich orthopyroxene and clinopyroxene that probably coexisted with olivine and Cr–Al spinel. This idea is further corroborated by the lack of spinel inclusions in garnet and by the absence of paired olivine and garnet inclusions in pyroxenes, which would be expected if garnet had not formed by exsolution but by reaction from spinel and pyroxenes at lower temperatures. Additionally, the compositional similarity of garnet and pyroxenes in all textural positions, as detailed below, further supports this interpretation. Similar textures observed in ultramafic *HP* rocks from various other localities have also been interpreted as being due to exsolution from former Al-rich *HT* pyroxenes (e.g. Dawson et al. 1980; Carswell 1986; Medaris and Carswell 1990).

Olivine grains in the matrix and olivine inclusions (ol I) in orthopyroxene are unzoned but show variable X_{Mg} of 0.768–0.793 (Table 1). The largest spinel inclusions in olivine are zoned with $Cr/(Cr + Al)(= X_{Cr})$ decreasing from 0.226 in cores (Table 1) to 0.152 at rims; the smaller inclusions have rather uniform X_{Cr} around 0.16. Orthopyroxene porphyroclasts (opx I) are bronzites with X_{Mg} of 0.821–0.846 and Al_2O_3 contents of 0.45–0.50 wt% (Table 1). At contacts with garnet inclusions (grt I), there is often a pronounced increase in Al_2O_3 (up to 6 wt%) and a slight decrease in X_{Mg} down to 0.800 (Fig. 3a). This rim composition is also displayed by tiny orthopyroxene inclusions in grt I (which is itself included in orthopyroxene prophyroclasts) and is interpreted to reflect late-stage partial re-equilibration as there are often narrow rims of amphibole between grt I and opx I (Fig. 3a). Clinopyroxene porphyroclasts and inclusions (cpx I) are Na_2O-poor diopsides with Al_2O_3 contents between 0.5 and 1.5 wt% and X_{Mg} between 0.907 and 0.926 (Table 1). Garnet I grains have 4.9–6.2 wt% CaO and X_{Mg} between 0.549 and 0.607 (Table 1). Within this range, they show irregular zoning patterns and tend to display a slight rimwards decrease in X_{Mg} and Ca contents at some of their contacts with surrounding opx I, due to the beginning formation of amphibole.

Table 1 Representative mineral compositions for garnet websterites. Formula calculations on the basis of 6 oxygens for cpx and opx, 4 oxygens for ol, 12 oxygens for grt, 4 oxygens and 3 cations for spl, and 15 cations without Na + K for amphiboles. X_{Mg} for grt, ol, opx, and cpx calculated on the assumption that all Fe is divalent; X_{Mg} for spl and amph is calculated using $Fe^{2+}/(Fe^{2+} + Fe^{3+})$ ratio as given by formula calculation. For mineral abbreviations see section on textures, mineral compositions, and evolutionary stages. (NC not calculated, ND not determined)

Sample no.	OW-41	OW-41	OW-41	OW-41	OW-41	OW-41	OW-41	OW-41	OW-41	OW-41	OW-41	OW-41
Mineral	Opx I	Cpx I	Grt I	Ol I	Spl I	Opx II	Cpx II	Grt II	Spl II	Cpx III	Cpx III	Amph I
SiO_2	56.52	55.00	40.63	38.41	0.03	55.39	54.20	40.76	0.05	53.27	53.94	52.47
TiO_2	0.04	0.05	0.04	0.00	0.08	0.10	0.07	0.04	0.00	0.09	0.11	0.25
Al_2O_3	0.50	0.57	22.20	0.00	45.67	1.66	1.12	22.71	64.60	3.10	1.01	7.49
Cr_2O_3	0.01	0.02	0.47	0.07	17.59	0.09	0.17	0.01	0.90	0.08	0.00	0.17
Fe_2O_3	NC	NC	NC	NC	2.91	NC	NC	NC	0.97	NC	NC	1.48
FeO	10.55	3.06	16.70	21.18	21.33	11.28	3.53	16.87	16.11	14.67	3.18	3.11
MnO	0.01	0.02	0.36	0.28	0.21	0.05	0.06	0.61	0.09	0.34	0.11	0.02
NiO	ND	ND	ND	0.00	ND	ND	ND	ND	ND	ND	ND	ND
MgO	32.03	17.64	14.46	40.03	11.38	31.17	17.25	14.35	16.89	28.25	17.18	19.63
CaO	0.28	23.48	5.15	0.03	0.00	0.30	23.36	4.96	0.12	0.23	24.66	12.86
Na_2O	0.02	0.34	0.00	0.00	0.00	0.01	0.33	0.00	0.01	0.02	0.13	0.08
K_2O	0.00	0.00	0.00	0.00	0.00	0.00	0.00	0.00	0.00	0.00	0.00	0.05
H_2O[a]												2.17
Total	99.96	100.18	100.01	100.00	99.20	100.05	100.09	100.31	99.74	100.05	100.32	99.78
Si	1.984	1.994	3.001	0.994	0.001	1.952	1.974	2.999	0.001	1.912	1.964	7.261
Ti	0.001	0.001	0.002	0.000	0.002	0.003	0.002	0.002	0.000	0.002	0.003	0.026
Al	0.021	0.024	1.933	0.000	1.537	0.069	0.048	1.970	1.961	0.131	0.043	1.221
Cr	0.000	0.000	0.028	0.001	0.397	0.002	0.001	0.001	0.018	0.002	0.000	0.019
Fe^{3+}	NC	NC	NC	NC	0.063	NC	NC	NC	0.019	NC	NC	0.154
Fe^{2+}	0.310	0.093	1.031	0.458	0.509	0.332	0.108	1.038	0.347	0.440	0.097	0.360
Mn	0.000	0.001	0.023	0.006	0.005	0.001	0.002	0.038	0.002	0.010	0.003	0.002
Ni	ND	ND	ND	0.000	ND	ND	ND	ND	ND	ND	ND	ND
Mg	1.677	0.954	1.592	1.544	0.484	1.638	0.937	1.574	0.648	1.511	0.933	4.049
Ca	0.010	0.912	0.407	0.001	0.000	0.011	0.912	0.391	0.003	0.009	0.962	1.907
Na	0.001	0.024	0.000	0.000	0.001	0.000	0.023	0.000	0.000	0.001	0.009	0.022
K	0.000	0.000	0.000	0.000	0.000	0.000	0.000	0.000	0.000	0.000	0.000	0.009
Total	4.004	4.003	8.017	3.004	2.999	4.008	4.007	8.013	2.999	4.018	4.014	15.030
X_{Mg}	0.844	0.911	0.607	0.771	0.458	0.831	0.897	0.603	0.639	0.774	0.906	0.918

[a] Calculated on the assumption of 2 OH per formula unit

In particular the marginal parts of opx I porphyroclasts have often recrystallized to smaller polygonal orthopyroxene grains (opx II) free of inclusions that coexist with small clinopyroxene (cpx II) and garnet grains (grt II), together forming a granoblastic texture (Fig. 2a). Garnet II may form clusters and larger grains. This second generation of pyroxenes and garnet is compositionally indistinguishable from the first generation except that opx II tends to have higher Al_2O_3 contents and slightly lower X_{Mg} than opx I (Table 1).

Between grt II and ol I, symplectitic and corona-like intergrowths of pyroxenes and spinel, which may also grade into a granoblastic texture, have developed by the reaction ol I + grt II = opx III + cpx III + spl II (Fig. 2a). Orthopyroxene III is more ferriferous and has variable but constantly higher Al_2O_3 contents compared to earlier orthopyroxene generations (Table 1). Clinopyroxene III is compositionally indistinguishable from cpx II (Table 1). Spinel II is a pleonaste poor in Cr. Vermicular spinel and clinopyroxene with corresponding compositions (spl IIa and cpx IIIa) are also observed in opx I porphyroclasts at contact zones with grt I inclusions and are generated by the reaction opx I + grt I = opx III + spl IIa + cpx IIIa.

Magnesio-hornblende to tremolitic hornblende has formed in three textural sites. Small polygonal grains (amph I) sometimes form part of the mosaic texture with opx II, cpx II and grt II while larger grains seem to overgrow the latter. Amphibole I is also in textural equilibrium with cpx III and opx III (Table 1) and has further developed at contacts of opx I porphyroclasts with grt I inclusions (Fig. 3a) as well as along cracks in opx I. Moreover, hornblende forms part of the kelyphitic rims developed around garnet that further consist of Cr-poor spinel, orthopyroxene and plagioclase.

Considering the results of experiments on the stability and composition of pyroxenes in garnet peridotites and spinel peridotites (Green and Ringwood 1967; Kushiro et al. 1972; Brey and Köhler 1990; Canil 1991; Canil 1992) as well as the interpretation of similar rock textures observed in garnet-bearing pyroxenites and peridotites from other localities (Carswell 1973; Obata and Morten 1987), the textural relations and mineral compositions described above indicate the following stages of metamorphic evolution:

Stage 0: *HT* stage within the spinel peridotite stablility field, characterized by the coexistence of former Al-rich pyroxenes (opx 0, cpx 0) with olivine (ol I) and spinel (spl I).

Stage 1: *HP* stage within the garnet peridotite stability field, leading to the formation of garnet (grt I) and Al-poor pyroxenes (opx I, cpx I) coexisting with ol I.

Stage 2: Nearly isothermal decompression, resulting in recrystallization and partial re-equilibration at lower pressures (opx II + cpx II + grt II), possibly accompanied by the beginning of hydration (formation of small amph I grains).

Stage 3: Further decompression and hydration, characterized by the reactions grt II + ol I = opx III + cpx III + spl II, opx I + grt I = spl IIa + cpx IIIa, and by the formation of large amphibole blasts (amph I).

HO-2 Opx I	HO-2 Cpx I	HO-2 Grt I	HO-2 Opx II	HO-2 Cpx II	HO-2 Grt II	HO-2 Amph I
56.32	54.30	40.42	55.76	54.29	40.05	56.02
0.00	0.06	0.00	0.00	0.06	0.05	0.04
0.43	2.08	22.81	0.94	2.55	22.21	1.95
0.06	0.12	0.24	0.02	0.23	0.49	0.02
NC	NC	NC	NC	NC	NC	0.26
11.54	4.52	17.33	12.49	3.92	18.71	5.00
0.15	0.09	0.44	0.08	0.02	0.52	0.09
ND	ND	ND	ND	ND	ND	ND
31.21	16.26	14.30	30.55	15.77	12.44	22.45
0.21	21.47	4.32	0.23	21.95	5.71	11.56
0.04	1.12	0.01	0.02	1.26	0.00	0.54
0.00	0.02	0.00	0.00	0.00	0.00	0.20
						2.17
99.96	100.04	99.87	100.09	100.05	100.18	100.30
1.987	1.978	2.989	1.973	1.974	2.989	7.733
0.000	0.002	0.000	0.000	0.002	0.003	0.004
0.018	0.089	1.988	0.039	0.109	1.954	0.318
0.002	0.004	0.014	0.001	0.007	0.029	0.002
NC	NC	NC	NC	NC	NC	0.027
0.340	0.138	1.072	0.370	0.119	1.168	0.577
0.005	0.003	0.027	0.002	0.001	0.033	0.010
ND	ND	ND	ND	ND	ND	ND
1.642	0.883	1.576	1.612	0.855	1.384	4.620
0.008	0.838	0.342	0.009	0.089	0.457	1.710
0.002	0.079	0.001	0.002	0.000	0.000	0.145
0.000	0.001	0.000	0.000	0.000	0.000	0.035
4.004	4.015	8.009	4.008	4.006	8.017	15.181
0.828	0.865	0.595	0.813	0.878	0.542	0.889

Further stages of decompression, cooling, and hydration include the formation of kelyphite from garnet and the formation of serpentine and magnetite from olivine.

Garnet websterite HO-2

The rock is fine grained and compositionally heterogeneous. It consists of clinopyroxene, orthopyroxene, garnet, Ca-amphibole, and of minor plagioclase, spinel, rutile, magnetite, and zircon. Some parts are characterized by extensive growth of tremolitic amphibole leading to the local formation of amphibole felses.

Within the less amphibolized parts, textures are similar to those of OW-41, except that olivine is absent. Again there is a relic texture with large orthopyroxene porphyroclasts (opx I) containing inclusions of garnet (grt I) and clinopyroxene (cpx I) (Fig. 2b), interpreted in the same way as for sample OW-41. Orthopyroxene I grains are bronzites with X_{Mg} between 0.810 and 0.835 and Al_2O_3 contents of 0.30–0.50 wt% (Table 1), displaying a similar compositional zoning at contacts with grt I as described for sample OW-41. Clinopyroxene I has higher Na_2O (1.0 – 2.5 wt%) and Al_2O_3 contents (1.0 – 2.5 wt%) than in OW-41 (Table 1). Garnet I has X_{Mg} between 0.541 and 0.600 and CaO contents between 4.7 and 6.5 wt% (Table 1). Larger grt I grains show irregular zoning of Ca, Mg, and Fe within the range given above (Fig. 3b). Most of them display a decrease in X_{Mg} towards their rims which is best explained by the formation of kelyphites consisting of fine-grained spinel, orthopyroxene, plagioclase, and amphibole.

As in the case of sample OW-41, there is a second texture defined by small polygonal grains of cpx II, opx II and grt II (Table 1), with grt II forming either poikiloblastic aggregates with numerous inclusions of clinopyroxene and rutile or small clear grains (Fig. 2b). Within the compositional range of grt I, grt II grains tend to have slightly lower X_{Mg} as well as higher Ca and Cr contents on the average (Table 1). Clinopyroxene II shows the same compositional features as cpx I, while opx II is enriched in Al compared to opx I (Table 1). This granoblastic texture II is overgrown by large tremolite blasts (amph I, Table 1).

Apart from the fact that no olivine is present, the metamorphic evolution of garnet websterite HO-2 is very similar to that of the garnet-olivine websterite OW-41 described above.

Garnet-spinel peridotite HH-10

Discrete shear zones rich in late-stage talc, chlorite, serpentine, graphite, and magnetite separate less foliated and more relic rock portions in which orthopyroxene (opx I), clinopyroxene (cpx I), olivine (ol I), garnet (grt I), Cr-Al spinel (spl I), and pargasitic hornblende (amph I) seem to have been in textural equilibrium. Orthopyroxene I, cpx I, and amph I occur as unoriented blasts of variable size.

Garnet I grains contain inclusions of opx I, cpx I, spl I, amph I, and ol I. Along contacts between garnet and enclosed opx I and spl I, symplectites of magnesio-hornblende (amph IV) and Cr-poor spinel (spl III), between 5 and 20 μm wide, have developed. Similar amphibole-spinel symplectites containing additional orthopyroxene (opx II) occur between grt I and cpx I inclusions.

Round aggregates (Fig. 2c), consisting of decussate chlorite (chl) flakes, tremolite (amph II) and a few grains of calcite and brown Cr-rich spinel (spl II) are interpreted as pseudomorphs after grt I. Clinopyroxene I grains located near these pseudomorphs are often fringed by secondary tremolite or tremolitic hornblende (amph III).

Garnet I grains are rimmed by kelyphites consisting of fibrous magnesio-hornblende (amph V), Cr-poor spinel (spl IV), and orthopyroxene (opx III). These kelyphite rims are thickest along contacts with olivine from which they are separated by a seam of granoblastic orthopyroxene (opx IV). Formation of these kelyphites and opx IV seams took place after the transformation of some of the garnet grains to the chlorite-tremolite-spinel-calcite aggregates described above.

Serpentinization of olivine and orthopyroxene was accompanied by the formation of magnetite and graphite. Talc mainly formed along shear zones. No anthophyllite was found.

Individual grt I grains are comparatively homogeneous, but there is some compositional variation among the grains (Table 2). Towards kelyphitic rims and towards symplectites at contacts with pyroxene inclusions, grt I grains show compositional zoning (up to 60 μm wide) with increasing Fe and Mn and decreasing Mg contents (Fig. 4a).

Clinopyroxene I in the matrix is fairly homogeneous. The X_{Mg} ranges from 0.940 to 0.953. Some grains show a moderate decrease in Al_2O_3 and Cr_2O_3 contents from centre to edge. The Al_2O_3 contents range from 1.45 and 0.45 wt% but are mostly between 1.2 and 0.8 wt%. The CaO contents are between 24.0 and 24.9 wt%. The Cr_2O_3 (0.14–0.69 wt%) and Na_2O contents (0.17–0.49 wt%) are weakly correlated. Compositions of cpx I grains enclosed in garnet are similar to those of the matrix. Some of these grains additionally exhibit a minor increase in Al_2O_3 and Cr_2O_3 and a decrease in MgO towards symplectites separating them from their garnet hosts.

Matrix opx I grains locally also show compositional zoning with Al_2O_3 (0.88–2.10 wt%) decreasing from core to rim. In some grains a negligible decrease in FeO and CaO along with an increase in MgO was found. The CaO contents are generally low (0.16–0.30 wt%) and X_{Mg} ranges from 0.898 to 0.909. Orthopyroxene I grains forming inclusions in garnet have compositions

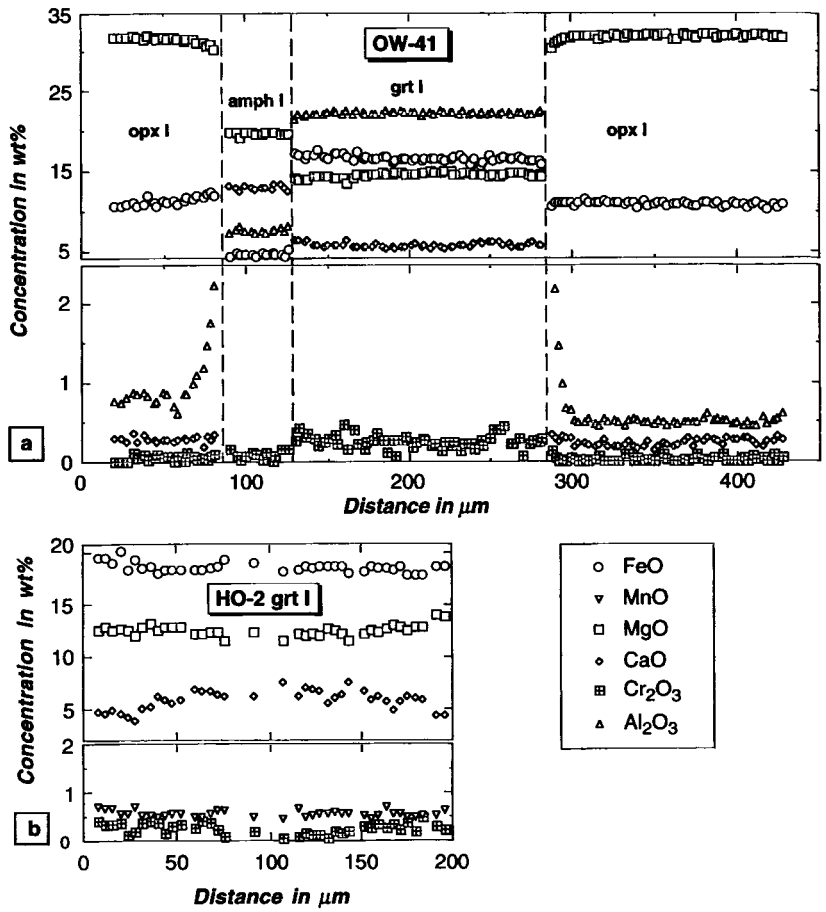

Fig. 3a, b Selected microprobe traverses from garnet websterites. **a** OW-41: contacts between inclusion of grt I in large porphyroclast of opx I. Along the contact to the *left*, secondary amphibole (*amph I*) has formed. Towards the grt I inclusion to the *right* as well as towards amph I, opx I shows a pronounced increase in Al_2O_3, a moderate increase in FeO, and a decrease in MgO. **b** HO-2: irregular zoning in large grt I grain included in opx I porphyroclast

similar to those of the matrix. Some of these grains, however, show an increase in FeO and a decrease in MgO towards the symplectite developed at the contact with garnet (Fig. 4a). Orthopyroxene II (symplectites between grt I and inclusions of cpx I) has higher Al_2O_3 contents (3.86 wt%) and lower X_{Mg} (0.819) than opx I. Orthopyroxene III (kelyphites) is characterized by Al_2O_3 contents around 3.0 wt% and X_{Mg} of about 0.88 (Table 2). Orthopyroxene IV grown at the outside of kelyphitic rims towards olivine has variable X_{Mg} (0.847–0.901) and Al_2O_3 contents (0.87–2.21 wt%).

The X_{Mg} of larger olivine grains (ol I) ranges from 0.876 to 0.903. Smaller olivine grains bordering kelyphite or secondary orthopyroxene near kelyphite (ol II) have lower X_{Mg} (0.856–0.876).

The X_{Cr} and X_{Mg} of primary spinel grains are variable (0.369–0.595 and 0.582–0.390, respectively) and are inversely correlated. Spinel grains included in garnet (spl I g) have lower X_{Cr} for any given X_{Mg} than spinel grains of the matrix or those enclosed in opx I and amph I (spl I m) (Fig. 5a). Individual spl I grains may be zoned with X_{Cr} increasing and X_{Mg} decreasing from core to rim, intra-grain variation being smaller than variation among individual grains. Spinel II occurring in pseudomorphs after grt I shows X_{Cr}-X_{Mg} relationships similar to spl I g (Table 2). Spinel III (symplectites) and spl IV (kelyphites) are Cr-poor pleonastes with X_{Mg} ranging from 0.647 to 0.736.

Amphibole I is a pargasitic hornblende with X_{Mg} ranging from 0.912 to 0.924 (Table 2). Amphibole II (pseudomorphs after grt I) and amph III (fringing cpx I) vary in composition from tremolite to tremolitic hornblende (Table 2). Amphibole IV (symplectites between grt and inclusions of cpx I, opx I and spl I) and amph V (kelyphite) are magnesio-hornblendes characterized by lower X_{Mg} compared to amph I and II. The composition of chl is close to clinochlor (Table 2).

Garnet-spinel peridotite KA-1

Although this rock is considerably serpentinized, the amount and preservational state of relic minerals allow us to assess original textures. Under the microscope, the rock exhibits a weak foliation, mainly defined by stretched garnet porphyroblasts (up to 5 mm in length; grt I) and associated strings of primary Cr-Al spinel (spl I) (Fig. 2d). Primary orthopyroxene (opx I), clinopyroxene (cpx I), olivine (ol I), and minor amphibole (amph I) are recrystallized to a great extent and it is generally not possible to distinguish between porphyroclasts and neoblasts.

Garnet contains inclusions of spl I, opx I, cpx I, and amph I and is partly transformed to a kelyphite consisting of amphibole (amph II) and Cr-poor spinel (spl II). Towards olivine, this kelyphite is bordered by a thin corona of orthopyroxene (opx II), minor clinopyroxene (cpx II), and rare amphibole (amph III). Although mainly associated with garnet, spl I also occurs in the matrix and is partly included in opx I, cpx I, and ol I. Opx I and cpx I do not show exsolution lamellae and there is no difference in chemical composition between neoblasts and rare porphyroclasts.

Individual grt I grains appear to be rather homogeneous, but there is a minor compositional variation from grain to grain. The X_{Mg} and CaO range from 0.740 to 0.808 and 5.41 to 7.84 wt%, respectively. A representative garnet composition is given in Table 2. Towards cracks and kelyphitic rims of the grains, compositional zoning with increasing Fe and Mn and decreasing Mg abundances may occur.

There is no systematic compositional difference between cpx I grains in the matrix and those enclosed in garnet. The Al_2O_3 contents range from 0.49 to 1.26 wt% but are mostly below 1.05 wt%. The CaO contents are high and vary between 23.6 and

24.9 wt%. The Na_2O (0.17–0.49 wt%) and Cr_2O_3 contents (0.14–0.55 wt%) are weakly correlated. The X_{Mg} ranges from 0.936 to 0.959. Larger cpx I grains show an increase in Al and a decrease in Cr and Na from core to rim, whilst Ca, Fe, and Mg remain constant (Fig. 4b). Clinopyroxene II grown at the outside of kelyphites tends to have lower X_{Mg} than cpx I (Table 2).

From cores to rims, opx I grains show increasing Al_2O_3 (0.60–2.00 wt%), Cr_2O_3 (0.04–0.30 wt%), and FeO (5.26–7.25 wt%), but decreasing MgO (34.3–36.4 wt%). The CaO contents are generally low (0.16–0.27 wt%) and do not vary systematically from core to rim. The X_{Mg} ranges from 0.895 to 0.923. Orthopyroxene II grains, grown at the outer margins of kelyphite rims towards olivine, have lower X_{Mg} (0.871–0.892) and lower Cr_2O_3 contents (< 0.10 wt%) than primary opx I.

The X_{Mg} of large olivine (ol I) grains ranges from 0.890 to 0.917, whilst olivines bordering kelyphite or secondary orthopyroxene (ol II) have lower X_{Mg} (0.868–0.889). The X_{Cr} and X_{Mg} of spl I grains are variable (0.365–0.540 and 0.635–0.437, respectively) and are inversely correlated (Fig. 5b). As in sample HH-10, spinel grains included in garnet tend to have lower X_{Cr} for any given X_{Mg} than spinel grains of the matrix or those included in other phases. Individual spinel grains may be zoned with X_{Cr} decreasing and X_{Mg} increasing from core to rim.

Amphibole I is a chromian magnesio-hornblende to tschermakitic hornblende with X_{Mg} ranging from 0.946 to 0.950. Kelyphitic amphiboles (amph II) are tremolitic hornblendes. Amphibole marginal to kelyphite (amph III) varies in composition from tremolite to tremolitic hornblende (Table 2).

Thermobarometry

Selection of thermometers and barometers

The *P-T* conditions for peridotite and pyroxenite mineral assemblages may be estimated by a variety of geothermobarometers. Accuracy of and systematic differences between most of the available formulations have been either tested empirically (Finnerty and Boyd 1987; Carswell and Harley 1990) or checked experimentally (Brey et al. 1990; Brey and Köhler 1990). The latter authors provide sets of thermometers and barometers that are able to reproduce experimental results or independently constrained temperatures and pressures quite well. These sets have therefore been used for this study.

Temperatures were calculated using formulations based on (1) the enstatite-diopside solvus (Brey and Köhler 1990; Bertrand and Mercier 1985 in a modified version as suggested by Brey and Köhler 1990); (2) the Fe-Mg distribution between garnet and clinopyroxene (Krogh 1988); (3) the Fe-Mg exchange between garnet and orthopyroxene (Brey and Köhler 1990); (4) the amount of Ca in orthopyroxene coexisting with garnet, olivine and clinopyroxene (Brey and Köhler 1990); (5) the Fe-Mg partitioning between garnet and olivine (O'Neill and Wood 1979). Pressures were calculated using the barometer of Brey and Köhler (1990), based on the amount of Tschermak's component in orthopyroxene coexisting with garnet. Maximum pressures for spinel-bearing assemblages were estimated from spinel compositions (Webb and Wood 1986). Since outermost rim compositions of most grains in all samples are modified by the formation of late-stage mineral phases, kelyphites and symplectites, only core and inner rim compositions were used for geothermobarometric calculations. The results are listed in Table 3 and are graphically presented in Fig. 6.

Garnet-olivine websterite OW-41

Spinel I core compositions calculated according to Webb and Wood (1986) indicate pressures of 1.7–2.3 GPa for assumed temperatures of 800–1300° C. These pressures are maximum pressures as they relate to the grt-in reaction and as this reaction is displaced towards lower pressures in Cr-poor and Fe-rich bulk systems (compared to average peridotites). Temperatures for stage 0 cannot be calculated as the pyroxenes of stage 0 are not preserved.

For stage 1, the three assemblages listed in Table 3 [(1) grt I + cpx I in opx I, ol I; (2) opx I, cpx I; (3) grt I in cpx I, ol I) yield the same temperatures and pressures within error limits. The *P-T* values calculated for the assemblage (1) are taken here for further discussion. Pressures calculated with the barometer of Brey and Köhler (1990) are 2.7 ± 0.3 GPa at 700° C and 3.3 ± 0.3 GPa at 800° C. Temperatures calculated according to different formulations show systematic variations. The two-pyroxene thermometers (Bertrand and Mercier 1985, modified version; Brey and Köhler 1990) as well as the Ca-in-orthopyroxene thermometer (Brey and Köhler 1990) given consistent temperatures of 789 ± 37, 816 ± 41, and 820 ± 24° C, respectively, at an assumed pressure of 3.0 GPa. The formulations based on Fe-Mg partitioning between garnet and orthopyroxene (Brey and Köhler 1990), and garnet and olivine (O'Neill and Wood 1979) yield consistently lower values (Table 3) of 704 ± 37° C and 695 ± 20° C and even lower (628 ± 17° C, Krogh 1988) for garnet-clinopyroxene.

Apart from the fact that the exchange equilibria used for thermometry have different blocking temperatures due to differing diffusion velocities of the involved components, the spread in calculated temperatures may have several reasons: (1) unconstrained extrapolation of high-temperature calibration data to temperatures below 900° C; (2) uncertainties in the oxidation state of Fe; (3) ferriferous bulk rock chemistry compared to the experimentally calibrated magnesian systems; (4) post-stage 1 readjustment of Fe and Mg to lower temperatures as at least in garnet these two elements are known to have the highest diffusion coefficients of all elements used for the *P-T* calculations applied (Elphick et al. 1985; Chakraborty and Ganguly 1992). As the different temperature calculations for sample HO-2 are sufficiently consistent at about 750° C, possibilities (2) and (4) seem to account best for the spread in temperatures obtained with Fe-Mg

Table 2 Representative mineral compositions for magnesian garnet-spinel peridotites. Formula calcuations on the basis of 6 oxygens for cpx and opx, 4 oxygens for ol, 12 oxygens for grt, 4 oxygens and 3 cations for spl, and 15 cations without Na + K for amphiboles X_{Mg} for grt, ol, opx, cpx, and chl calculated on the assumption that all Fe is divalent; X_{Mg} for spl and amph is calculated using $Fe^{2+}/(Fe^2 + Fe^{3+})$ ratio as given by formula calculation. For mineral abbreviations see section on textures, mineral compositions, and evolutionary stages. (*c* core, *r* rim, *g* inclusion in garnet, *m* matrix, *NC* not calculated, *ND* not determined)

Sample no.	HH-10	HH-10	HH-10	HH-10	HH-10	HH-10	HH-10	HH-10	HH-10	HH-10	HH-10	HH-10
Mineral	Opx I	Cpx I	Grt I	Ol I	Spl Ig	Spl Im	Amph I	Chl	Amph II	Amph III	Spl II	Amph IV
SiO_2	57.14	54.82	41.70	40.94	ND	ND	45.39	30.94	57.11	55.21	ND	51.23
TiO_2	0.05	0.07	0.04	0.02	0.33	0.59	0.48	0.11	0.03	0.21	0.30	0.17
Al_2O_3	1.15	0.68	22.13	0.00	23.50	23.95	11.95	18.12	1.41	3.59	25.23	9.31
Cr_2O_3	0.21	0.35	1.57	0.03	44.60	43.31	1.41	1.96	0.25	0.79	41.36	0.56
Fe_2O_3	NC	NC	NC	NC	0.05	0.00	0.24	NC	0.50	0.58	1.75	0.48
FeO	6.50	1.81	10.33	9.60	22.02	22.98	2.75	2.83	1.29	1.47	21.26	3.15
MnO	0.15	0.03	0.60	0.10	0.18	0.26	0.03	0.04	0.03	0.09	0.43	0.24
NiO	ND	ND	ND	0.29	ND	ND	ND	ND	ND	ND	ND	ND
MgO	34.96	17.68	17.64	49.45	9.01	8.48	19.23	32.68	23.36	22.19	9.52	19.75
CaO	0.18	24.12	6.02	0.00	0.00	0.00	12.42	0.06	13.15	13.19	0.00	11.72
Na_2O	0.00	0.37	0.02	0.00	ND	ND	2.33	0.00	0.09	0.22	ND	0.34
K_2O	0.00	0.00	0.00	0.00	ND	ND	0.82	0.00	0.01	0.01	ND	0.00
H_2O[a]							2.11	12.64	2.19	2.18		2.16
Total	100.33	99.91	100.05	100.43	99.69	99.57	99.16	99.38	99.42	99.73	99.85	99.11
Si	1.965	1.988	3.008	0.998	ND	ND	6.458	2.935	7.832	7.586	ND	7.118
Ti	0.001	0.002	0.002	0.000	0.008	0.014	0.052	0.008	0.003	0.021	0.007	0.018
Al	0.046	0.029	1.882	0.000	0.872	0.891	2.004	2.026	0.228	0.581	0.926	1.524
Cr	0.006	0.010	0.089	0.001	1.111	1.081	0.158	0.147	0.027	0.085	1.019	0.062
Fe^{3+}	NC	NC	NC	NC	0.001	0.000	0.026	NC	0.052	0.060	0.041	0.051
Fe^{2+}	0.187	0.055	0.623	0.196	0.580	0.607	0.327	0.224	0.148	0.169	0.554	0.366
Mn	0.004	0.001	0.036	0.002	0.005	0.007	0.003	0.003	0.003	0.010	0.011	0.029
Ni	ND	ND	ND	0.006	ND	ND	ND	ND	ND	ND	ND	ND
Mg	1.792	0.956	1.897	1.798	0.423	0.399	4.079	4.622	4.776	4.546	0.442	4.090
Ca	0.006	0.937	0.465	0.000	0.000	0.000	1.894	0.006	1.932	1.941	0.000	1.744
Na	0.000	0.026	0.003	0.000	ND	ND	0.643	0.000	0.023	0.058	ND	0.092
K	0.000	0.000	0.000	0.000	ND	ND	0.149	0.000	0.002	0.001	ND	0.000
Total	4.007	4.004	8.005	3.001	3.000	3.000	15.793	9.971	15.025	15.058	3.000	15.093
X_{Mg}	0.905	0.946	0.753	0.902	0.421	0.397	0.926	0.954	0.970	0.964	0.444	0.918

[a] Calculated on the assumption of 2 OH (amphibole) and 8 OH (chlorite) per formula unit

exchange thermometers for sample OW-41. Therefore, using the two-pyroxene thermometers (Bertrand and Mercier 1985, modified version; Brey and Köhler 1990) as well as the Ca-in-orthopyroxene thermometer (Brey and Köhler 1990), a graphically derived best fit range for pressures and temperatures seems to be between 3.2 and 3.6 GPa at 780–850° C (Fig. 6).

Mineral compositions of stage 2 are largely the same as for stage 1, except that Al abundances are significantly higher in opx II than in opx I. Additionally, there are strong variations in Al abundancies of opx II grains and all of the stage 2 phases tend to be compositionally inhomogeneous. Therefore, temperatures calculated for stage 2 assemblages largely coincide with those for stage 1 and pressures are significantly lower (1.4–1.9 GPa at 700 and 800° C, respectively), but there is a very large scatter in the data (Table 3).

Reliable *P-T* calculations for stage 3 are hampered by the small grain size of and concentration gradients within opx III, cpx III, and spl II in the symplectites developed between grt II and ol I. As the zoning patterns of garnet and the pyroxenes do not reflect heating during decompression (only minor changes in Fe/Mg ratios in garnet and pyroxenes along with significant increases of Al at orthopyroxene rims), temperatures should roughly coincide with those of stage 2.

Garnet-websterite HO-2

Stage 1 assemblages of sample HO-2 record similar *P-T* conditions as those of OW-41. As in the case of OW-41, the *P-T* values calculated for stage I from three different assemblages (Table 3) coincide. Again, the *P-T* values for the assemblage grt I + cpx I in opx I are taken for further discussion. In contrast to sample OW-41, there is a fairly good agreement between the values calculated with different thermometers (700–800° C, Table 3). The highest temperatures at an assumed pressure of 3.5 GPa are 800 ± 57° C and 792 ± 46° C, calculated with the modified version of the

HH-10 Spl III	HH-10 Opx II	HH-10 Opx III	HH-10 Opx IV	HH-10 Amph V	HH-10 Spl IV	HH-10 Ol II
ND	54.32	55.35	56.51	48.81	ND	40.16
0.01	0.03	0.03	0.06	0.15	0.00	0.02
64.65	3.86	2.94	1.56	12.12	61.02	0.00
2.32	0.21	0.21	0.03	1.35	5.36	0.00
0.28	NC	NC	NC	1.22	0.73	NC
12.77	11.73	7.95	8.94	3.48	14.41	13.66
0.14	0.47	0.30	0.47	0.24	0.25	0.41
ND	ND	ND	ND	ND	ND	0.46
19.01	29.72	33.41	32.80	17.57	17.50	46.07
0.00	0.21	0.14	0.07	12.30	0.00	0.05
ND	0.01	0.00	0.02	0.38	ND	0.00
ND	0.03	0.00	0.01	0.01	ND	0.00
				2.15		
99.18	100.59	100.33	100.47	99.78	99.27	100.83
ND	1.911	1.919	1.962	6.800	ND	0.996
0.000	0.001	0.001	0.002	0.015	0.000	0.000
1.947	0.160	0.120	0.064	1.990	1.875	0.000
0.047	0.006	0.006	0.001	0.148	0.110	0.000
0.005	NC	NC	NC	0.128	0.014	0.000
0.273	0.345	0.231	0.260	0.406	0.314	0.283
0.003	0.014	0.009	0.014	0.028	0.006	0.009
ND	ND	ND	ND	ND	ND	0.009
0.724	1.559	1.727	1.698	3.649	0.680	1.704
0.000	0.008	0.005	0.003	1.835	0.000	0.001
ND	0.001	0.000	0.000	0.102	ND	0.000
ND	0.001	0.000	0.000	0.001	ND	0.000
3.000	4.006	4.017	4.004	15.103	3.000	3.003
0.726	0.819	0.882	0.867	0.900	0.684	0.857

thermometer of Bertrand and Mercier (1985) and with the Ca-in-orthopyroxene thermometer of Brey and Köhler (1990), respectively. Within error limits they coincide with the temperatures calculated using the garnet-orthopyroxene thermometer of Brey and Köhler (1990) and the Krogh (1988) thermometer (736 ± 39° C and 734 ± 32° C, respectively). Temperatures calculated with the two-pyroxene thermometer of Brey and Köhler (1990) show a very strong scatter around 753 ± 88° C, most likely due to the Na sensitivity of this thermometer and the considerable scatter in Na contents of cpx I. The Al-in-opx pressures are 4.1 ± 0.3 GPa (Brey and Köhler 1990) at 800° C and 3.3 ± 0.3 GPa at 700° C. The graphical presentation (Fig. 6) shows a best fit range for calculated pressures and temperatures between about 3.6 and 4.3 GPa at 740–830° C.

The *P-T* conditions calculated for stage 2 also show a very strong scatter in both temperatures and pressures due to inhomogeneous phase compositions. Temperatures and pressures scatter around 750° C and 3.0 GPa, respectively.

Garnet-spinel peridotite HH-10

At low temperatures, i.e. below about 800° C, thermometers based on the Fe-Mg exchange between clinopyroxene and garnet (Krogh 1988) or olivine and garnet (O'Neill and Wood 1979; Brey and Köhler 1990, Fig. 1) are thought to be more reliable than those based on the steep diopside-enstatite solvus. We therefore combined the thermometer of Krogh (1988) with the orthopyroxene-garnet barometer of Brey and Köhler (1990) and obtained $T = 678 \pm 27°$ C/P $= 1.43 \pm 0.23$ GPa as best estimate for the equilibration conditions of this peridotite (cores of matrix grt I, cpx I, opx I; Table 3). Applying the two-pyroxene thermometer of Brey and Köhler (1990) yields temperatures of 629 ± 55° C (at 1.5 GPa). Calcium-in-orthopyroxene temperatures (Brey and Köhler 1990), however, are significantly higher (750 ± 18° C at 1.5 GPa). We also calculated temperatures for the Fe-Mg partitioning between orthopyroxene and garnet by using the formulation given by Brey and Köhler (1990, Fig. 1) and obtained 731 ± 61° C (at 1.5 GPa). The large spread in temperatures (617 ± 199° C at 1.5 GPa) obtained with the thermometer based on the Fe-Mg partitioning between olivine and garnet (O'Neill and Wood 1979) is possibly caused by partial re-equilibration of olivine during retrograde reactions (e.g. serpentinization). Temperatures calculated for coexisting garnet and clinopyroxene rims with the thermometer of Krogh (1988) coincide with those estimated for cores.

Garnet-spinel peridotite KA-1

Combination of the garnet-clinopyroxene Fe-Mg partitioning thermometer of Krogh (1988) with the orthopyroxene-garnet barometer of Brey and Köhler (1990) yielded $T = 732 \pm 26°$ C/P $= 1.77 \pm 0.19$ GPa for the cores of matrix pyroxenes and garnets (Table 3). By applying the two-pyroxene and Ca-in-orthopyroxene thermometers of Brey and Köhler (1990), temperatures of 702 ± 35° C and 741 ± 19° C, respectively, (at 1.5 GPa) were obtained. Similar temperatures of 709 ± 41° C were calculated on the basis of Fe-Mg partitioning between orthopyroxene and garnet by using the formulation of Brey and Köhler (1990, Fig. 1). As for sample HH-10, temperatures based on the Fe-Mg partitioning between garnet and olivine (O'Neill and Wood 1979) show a large spread (652 ± 182° C at 1.5 GPa).

Using core compositions of pyroxene inclusions in garnet we obtained $T = 735 \pm 34°$ C and $P = 1.87 \pm 0.27$ GPa (Table 3) for the combination of the thermometer of Krogh (1988) with the barometer of Brey and Köhler (1990). Similar temperatures of 728 ± 21° C, 772 ± 59° C, and 724 ± 34° C (at 1.5 GPa) were obtained by using the Ca-in-orthopyroxene (Brey and Köhler 1990), garnet-orthopyroxene (Brey and

Table 2 (continued)

Sample no.	Ka-1	Ka-1	Ka-1	Ka-1	Ka-1	Ka-1	Ka-1	Ka-1	Ka-1	Ka-1	Ka-1	Ka-1	Ka-1	Ka-1	Ka-1
Mineral	Opx Ic	Opx Ir	Cpx Ic	Cpx Ir	Grt 1	Ol 1	Spl Ic	Spl Ir	Amph I	Amph II	Amph II	Spl II	Opx II	Cpx II	Ol II
SiO_2	57.70	57.06	54.82	54.50	42.02	40.88	ND	ND	45.92	54.64	56.19	ND	56.34	54.52	40.20
TiO_2	0.05	0.07	0.03	0.10	0.05	0.01	0.36	0.07	0.36	0.19	0.05	0.04	0.04	0.04	0.00
Al_2O_3	0.60	1.67	0.61	0.92	22.44	0.01	25.55	32.72	12.39	5.19	2.39	65.18	1.46	0.69	0.01
Cr_2O_3	0.04	0.21	0.54	0.30	1.64	0.00	43.30	35.58	1.53	0.64	0.34	2.91	0.02	0.36	0.02
Fe_2O_3	NC	NC	NC	NC	NC	NC	0.85	0.54	1.98	0.97	2.04	0.53	NC	NC	NC
FeO	5.52	6.26	1.82	1.78	8.93	8.46	21.42	19.25	1.75	1.67	0.40	9.39	8.27	2.18	12.40
MnO	0.15	0.11	0.15	0.15	0.41	0.11	0.34	0.22	0.11	0.11	0.08	0.12	0.50	0.12	0.38
NiO	ND	ND	ND	ND	ND	0.40	ND	ND	ND	ND	ND	ND	ND	ND	0.42
MgO	35.88	35.08	17.74	18.05	18.87	50.86	9.95	11.60	18.44	21.69	23.29	21.33	33.23	18.02	47.18
CaO	0.19	0.22	23.85	23.88	6.25	0.00	0.01	0.06	12.56	12.94	12.97	0.08	0.20	23.69	0.03
Na_2O	0.00	0.01	0.49	0.28	0.00	0.00	ND	ND	1.38	0.10	0.05	ND	0.02	0.31	0.00
K_2O	0.00	0.00	0.02	0.00	0.00	0.00	ND	ND	0.55	0.03	0.01	ND	0.00	0.00	0.00
H_2O^a									2.12	2.20	2.20				
Total	100.13	100.69	100.07	99.96	100.61	100.73	101.78	100.04	99.09	100.37	100.01	99.58	100.08	99.93	100.64
Si	1.978	1.953	1.987	1.987	2.995	0.990	ND	ND	6.499	7.463	7.672	ND	1.960	1.980	0.994
Ti	0.001	0.002	0.001	0.003	0.003	0.000	0.008	0.001	0.038	0.020	0.005	0.001	0.001	0.001	0.000
Al	0.024	0.067	0.026	0.039	1.885	0.000	0.919	1.148	2.067	0.835	0.385	1.931	0.060	0.029	0.000
Cr	0.001	0.006	0.015	0.009	0.092	0.000	1.045	0.837	0.171	0.069	0.037	0.058	0.000	0.010	0.000
Fe^{3+}	NC	NC	NC	NC	NC	NC	0.020	0.012	0.211	0.100	0.210	0.010	NC	NC	NC
Fe^{2+}	0.158	0.179	0.055	0.054	0.532	0.171	0.547	0.479	0.207	0.191	0.045	0.197	0.241	0.066	0.256
Mn	0.005	0.003	0.005	0.005	0.025	0.002	0.009	0.006	0.013	0.013	0.010	0.003	0.015	0.004	0.008
Ni	ND	ND	ND	ND	ND	0.008	ND	ND	ND	ND	ND	ND	ND	ND	0.008
Mg	1.834	1.790	0.958	0.975	2.005	1.837	0.453	0.515	3.890	4.417	4.740	0.799	1.724	0.975	1.738
Ca	0.007	0.008	0.926	0.928	0.477	0.000	0.000	0.002	1.904	1.893	1.897	0.002	0.007	0.922	0.001
Na	0.000	0.000	0.034	0.019	0.000	0.000	ND	ND	0.378	0.027	0.012	ND	0.001	0.022	0.000
K	0.000	0.000	0.001	0.000	0.000	0.000	ND	ND	0.100	0.004	0.001	ND	0.000	0.000	0.000
Total	4.008	4.008	4.008	4.008	8.014	3.009	3.000	3.000	15.478	15.032	15.014	3.000	4.009	4.010	3.005
X_{Mg}	0.921	0.909	0.946	0.948	0.790	0.915	0.453	0.518	0.949	0.959	0.990	0.802	0.878	0.936	0.872

Köhler 1990, Fig. 1), and garnet-clinopyroxene (Krogh 1988) thermometers, respectively. Applying the thermometer of Krogh (1988) to coexisting garnet-clinopyroxene rims yielded slightly lower temperatures of 678 ± 25° C (at 1.5 GPa).

Discussion

P-T evolution of websterites and peridotites

Though not preserved as a mineral assemblage, a *HT* stage (stage 0) within the spinel peridotite stability field and subsequent exsolution of garnet from pyroxenes have been deduced from textures and mineral compositions for the websterites. A state 0 at comparatively low temperatures within the spinel peridotite stability field and subsequent formation of garnet by the reaction spl + opx + cpx = grt + ol have been rendered unlikely on the basis of inclusion relations. Thus, provided that postulated stage-0 *HT* Al-rich pyroxenes coexisted with the spinel inclusions in olivine, a large *P-T* range of 1.7–2.3 GPa/800–1300° C (Webb and Wood 1986) is possible. In ferriferous and Cr-poor bulk systems, the transition from spinel to garnet peridotite occurs at significantly lower pressures than in Mg-Cr peridotites (see compilation in Harley and Carswell 1990). This should restrict the possible pressure range for stage 0 to values below 1.3 and 1.5 GPa (Jenkins and Newton 1979; Gasparik 1987). Assuming further a cumulate origin for the websterites, consistent with their bulk chemistry and with current petrogenetic models for pyroxenites (Frey 1980; Irving 1980, Loubet and Allègre 1982), stage 0 minerals must have crystallized above the solidus, which is around 1300° C at the constrained pressures in vapour-absent Mg-rich bulk systems (Green and Ringwood 1967; Herzberg et al. 1990; Takahashi 1990).

For stage 1, temperatures between 740 and 850° C at pressures of 3.2–4.3 GPa were calculated. Thus, subsequent to their crystallization within the spinel peridotite stability field, the websterites were subject to cooling and compression. As stage 0 was most likely an igneous event, temperatures were probably local and tansient. Therefore, stage 0 does not represent a point on a *P-T* path in terms of having implications for environmental *P-T* conditions. Thus, the actual path (clockwise or anticlockwise) of the websterites between stage 0 and stage 1 cannot be constrained. Nevertheless, the rocks must have been cooled and taken down to depths of 100 to 120 km (stage 1). This is best explained by a tectonic setting where the websterites-

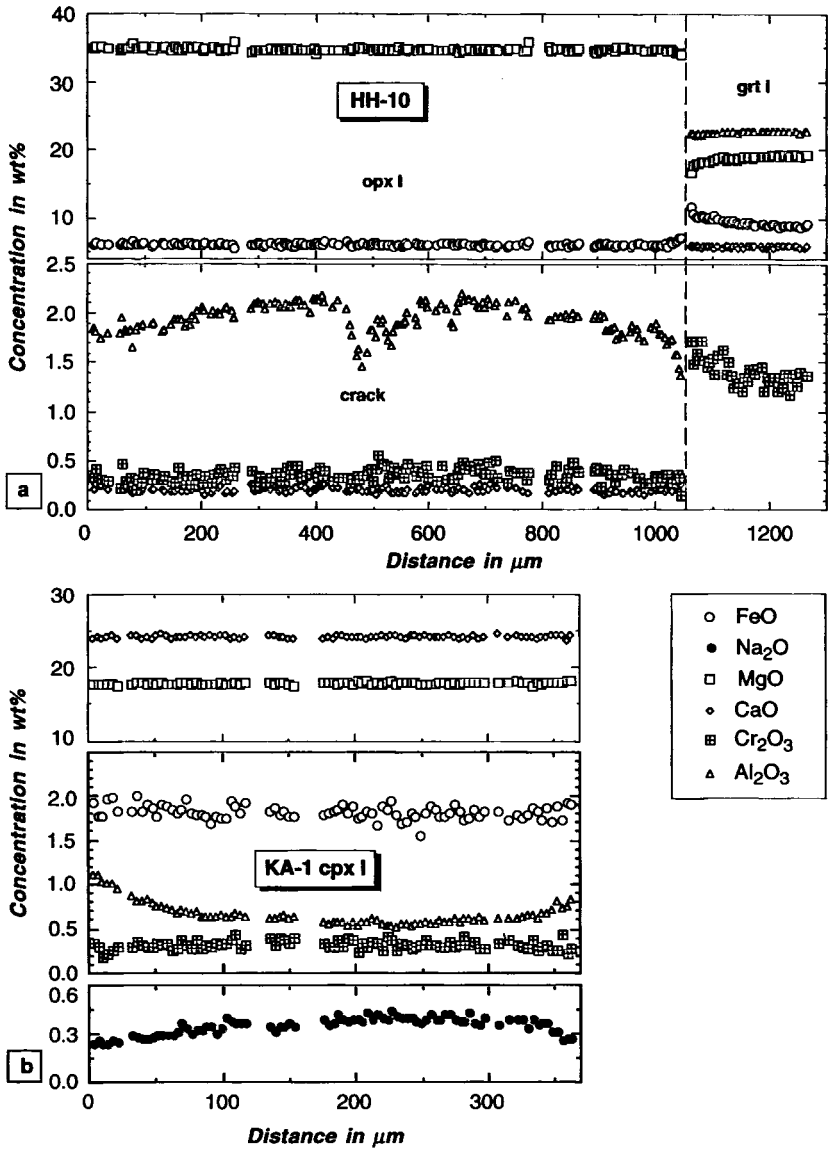

Fig. 4a, b Selected microprobe traverses from garnet-spinel peridotites. **a** HH-10: large inclusion of opx I in grt I showing constant MgO, FeO, CaO and Cr_2O_3, but decreasing Al_2O_3 from core to rim. Lower Al_2O_3 contents in the central part of this opx I grain are interpreted as secondary effects. Note that in both opx I and grt I MgO decreases and FeO increases towards the contact. Grt I also shows increasing Cr_2O_3 towards opx I. **b** KA-1: large cpx I grain showing an increase in Al_2O_3 and a decrease in Cr_2O_3 and Na_2O from core to rim

formed part of a hot continental lithosphere that was buried in the course of a continent-continent collision.

Subsequent decompression through stages 2 and 3 was nearly isothermal, as indicated by temperature estimates on stage 2 assemblages and by the flat slope of the reaction curve grt + ol = cpx + opx + spl in *P-T* space at temperatures around 800° C (stage 3). The websterites must have passed stages 2 and 3 too quickly for a severe re-equilibration. This is indicated by the preservation of stage-1 low-Al plateaus (Fig. 3) in large orthopyroxenes (up to several mm in diameter), by only very narrow high-Al rims of these stage 1 orthopyroxenes (Fig. 3), by inhomogeneous Al contents of the smaller orthopyroxenes grown during stage 2, as well as by comparatively thin stage 3 kelyphite rims around garnet.

For the garnet-spinel peridotites, equilibration conditions recorded are those of the garnet-spinel peridotite stability field as indicated by the presence of spinel both in the matrix and as inclusions in garnet, as well as by *P-T* calculations. As spinel is included in garnet (meaning that garnet grew at the expense of spinel), these rocks must have passed through the spinel peridotite stability field to higher pressures. This cannot have been accompanied by significant cooling (as in the case of websterites) since relics of an older H*T* stage are lacking in the pyroxenes. Further, as neither an older equilibration at higher *P-T* conditions nor a later re-equilibration at lower temperatures and pressures is recorded, the garnet-spinel peridotites must have resided in the garnet-spinel peridotite stability field for a comparatively long time.

In sample HH-10, minor pargasite was in stable association with the other minerals. Nevertheless, a_{H_2O} was probably small since opx + ol + spl was a stable assemblage at the rather low temperatures of

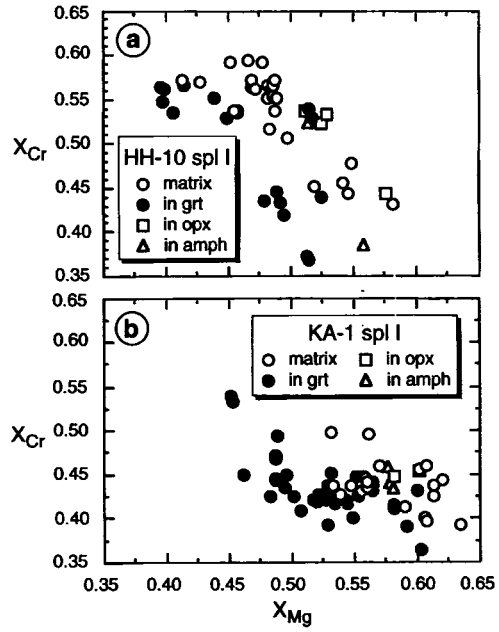

Fig. 5 X_{Cr} versus X_{Mg} of spl I in garnet-spinel peridotites HH-10 (**a**) and KA-1 (**b**). Note that for any given X_{Cr}, spl I included in grt I has lower X_{Mg} than spl I grains occurring in the matrix or as inclusions in other minerals

about 700° C as deduced from thermobarometry on garnet and pyroxenes. Later replacement of some garnet grains by aggregates of chlorite, tremolite, Cr-rich spinel, and minor calcite suggests infiltration of H_2O-CO_2-rich fluids. Under conditions of elevated a_{H_2O}, the low-temperature part of the garnet-spinel lherzolite stability field is replaced by the chlorite peridotite and chlorite-amphibole peridotite fields (Jenkins 1981, 1983; Obata and Thompson 1981). Since anthophyllite is not present in the rock, the transition to the lower-temperature amphibole-chlorite-talc peridotite stability field probably took place under elevated pressures, i.e. above about 0.8 GPa (Jenkins 1981, 1983). Zoning patterns of some of the larger orthopyroxenes (i.e. decreasing Al from core to rim) and of some spinels (i.e. increasing X_{Cr} from core to edge) may also be interpreted as a consequence of cooling under nearly constant pressures, although the very moderate zoning (Fig. 4a) allows only for small changes in temperature. During later serpentinization, the H_2O-CO_2 fluids were reduced as documented by graphite flakes intergrown with serpentine.

In garnet-spinel peridotite KA-1, zoning patterns of primary pyroxenes (i.e. increasing Al from core to rim) and spinels (i.e. decreasing X_{Cr} from core to rim) are interpreted to result from decompression under falling temperatures. This is also indicated by slightly lower temperatures for coexisting garnet-clinopyroxene rims as compared to those obtained on core compositions. During this nearly isothermal decompression, H_2O-rich fluids infiltrated the rock and caused formation of an amphibole-spinel kelyphite around garnet and of secondary tremolite or tremolitic hornblende. Later on, the rock was serpentinized.

Pressures and temperatures calculated for the magnesian garnet-spinel peridotites fit very well with

Table 3 Temperature and pressure estimates for ultramafic HP rocks from the Schwarzwald. Errors correspond to 1σ. W & W86 = Webb and Wood (1986), B & M 85 = Bertrand and Mercier (1985), modified version according to Brey and Köhler (1990), B & K = 90 = Brey and Köhler (1990), Krogh 88 = Krogh (1988), ON & W 79 = O'Neill and Wood (1979).

Sample	Stage	Mineral assemblage	Pressures in GPa *at assumed temperature*	
			P_{max}spl (W & W 86)	*P* Al-in-opx (B & K 90)
OW-41			*T* = 800°C *T* = 1300°C	
	0	Spl in ol I	1.7 ± 0.3 2.3 ± 0.3	
				T = 700°C *T* = 800°C
	1	Grt + cpx I in opx I, ol I		2.7 ± 0.3 3.3 ± 0.3
	1	Opx I, Cpx I		
	1	Grt I in cpx I, ol I		
				T = 700°C *T* = 800°C
	2	Grt II, opx II, cpx II		1.4 ± 1.1 1.9 ± 1.2
HO-2				*T* = 700°C *T* = 800°C
	1	Grt 1 + cpx I in opx I		3.3 ± 0.3 4.1 ± 0.3
	1	Opx 1, cpx I		
	1	Grt I in cpx I		
				T = 700°C *T* = 800°C
	2	Grt II, opx II, cpx II		2.2 ± 1.1 2.9 ± 1.1
HH-10				*T* = 700°C *T* = 750°C
	1	Matrix grt I, cpx I, opx I, ol I		1.5 ± 0.2 1.8 ± 0.3
KA-1				*T* = 700°C *T* = 750°C
	1	Cores of matrix grt I, cpx I, opx I, ol I		1.6 ± 0.2 1.9 ± 0.2
	1	Cores of px I inclusions in grt I		1.7 ± 0.3 1.9 ± 0.3
	1–2	Rims of matrix grt I, cpx I, opx I, ol I		1.6 ± 0.2 1.9 ± 0.2

minimum pressures calculated for eclogites of the CSGC ($\geqq$ 1.6 GPa/670–750° C, Kalt et al. 1994b, and unpublished data). As in the case of these eclogites, a clockwise *P-T* path can be inferred for the magnesian peridotites as they experienced concomitant compression and heating, followed by decompression and cooling. Clockwise *P-T* paths are comparatively well understood and are thought to result from collision metamorphism and crustal thickening, followed by erosional exhumation and extensional thinning (Thompson and England 1984; Anderson et al. 1992; Searle et al. 1992). They are mainly followed by rocks forming part of the subducted lithosphere.

In summary, contrasting *P-T* evolutions for the websterites on one side and the garnet-spinel peridotites on the other emerge from textures, mineral compositions and *P-T* estimates. Apart from lacking evidence for an early *HT* stage in the garnet-spinel peridotites, the most significant difference is in equilibration pressures. Due to the spread in calculated temperatures for both groups of rocks, no significant difference in equilibration temperatures at maximum pressures can be detected, although there is a tendency for higher equilibration temperatures of the websterites. Despite their contrasting peak pressures and different pre-peak evolutions, both groups of rocks are characterized by equilibration conditions typical of subducted or buried lithosphere. As there is no geochemical evidence for an oceanic or a continental origin in either of the two groups, websterites and garnet-spinel peridotites may or may not have formed part of one single lithospheric segment during a subduction and/or collision process.

Geological implications

Although there is convincing tectonic and petrological evidence that CSGC and SSW are different basement units (see section on geological setting), there are only few constraints on the internal structure of these two units. An internal nappe character may be inferred for the CSGC from the fact that monotonous gneisses and migmatites contain eclogites as well as garnet peridotites and websterites while more variegated gneiss lithologies are obviously devoid of *HP* relics. On the other hand, the *HP*-bearing gneiss unit itself could up to now not be subdivided on the basis of *P-T* conditions and structures. According to previous field work and petrographic investigations (Stenger et al. 1989), the monotonous gneisses and migmatites hosting the *HP* rocks have all experienced similar *HT* metamorphic conditions at the same time (335–330 Ma, Kalt et al. 1994a). The age of *HP* metamorphism is slightly higher (337–332 Ma, Kalt et al. 1994b) and also seems to be the same throughout the *HP*-mineral-bearing gneiss unit. At least the eclogites which have all equilibrated at *P-T* conditions similar to those of the garnet-spinel peridotites display the same Sm-Nd mineral isochron ages as garnet websterite HO-2 (A. Kalt, in preparation).

Nevertheless, the contrasting *P-T* evolutions recorded by websterites on one side and peridotites on the other suggest that the gneiss unit hosting them is not uniform but may be a nappe pile of several distinct slices of lithosphere. An additional argument in favour of this model is that gneisses and migmatites themselves are obviously devoid of *HP* mineral assemblages

Temperatures in °C *at assumed pressure*

T 2px (B & M 85)	*T* 2px (B & K 90)	*T* Ca-in-opx (B & K 90)	*T* grt-opx (B & K 90)	*T* grt-cpx (Krogh 88)	*T* grt-ol (O'N & W 79)
P = 3 GPa	*P = 3 GPa*	*P = 3 GPa*	*P = 3 GPa*	*P = 3 GPa*	*P = 3 GPa*
789 ± 37	816 ± 41	820 ± 24	704 ± 37	628 ± 17	695 ± 20
802 ± 29	825 ± 36	828 ± 13			
				654 ± 71	717 ± 40
P = 2 GPa	*P = 2 GPa*	*P = 2 GPa*	*P = 2 GPa*	*P = 2 GPa*	
728 ± 35	680 ± 56	801 ± 19	754 ± 42	623 ± 29	
P = 3.5 GPa	*P = 3.5 GPa*	*P = 3.5 GPa*	*P = 3.5 GPa*	*P = 3.5 GPa*	
800 ± 57	753 ± 88	792 ± 46	736 ± 39	734 ± 32	
754 ± 62	695 ± 72	811 ± 36			
				686 ± 52	
P = 2 GPa	*P = 2 GPa*	*P = 2 GPa*	*P = 2 GPa*	*P = 2 GPa*	
743 ± 86	611 ± 74	770 ± 41	749 ± 91	662 ± 39	
P = 1.5 GPa	*P = 1.5 GPa*	*P = 1.5 GPa*	*P = 1.5 GPa*	*P = 1.5 GPa*	*P = 1.5 GPa*
663 ± 36	629 ± 55	750 ± 18	731 ± 61	679 ± 27	617 ± 199
P = 1.5 GPa	*P = 1.5 GPa*	*P = 1.5 GPa*	*P = 1.5 GPa*	*P = 1.5 GPa*	*P = 1.5 GPa*
714 ± 29	702 ± 29	741 ± 19	709 ± 41	723 ± 27	652 ± 182
		728 ± 21	772 ± 59	724 ± 34	
722 ± 32	709 ± 40	742 ± 40		678 ± 25	

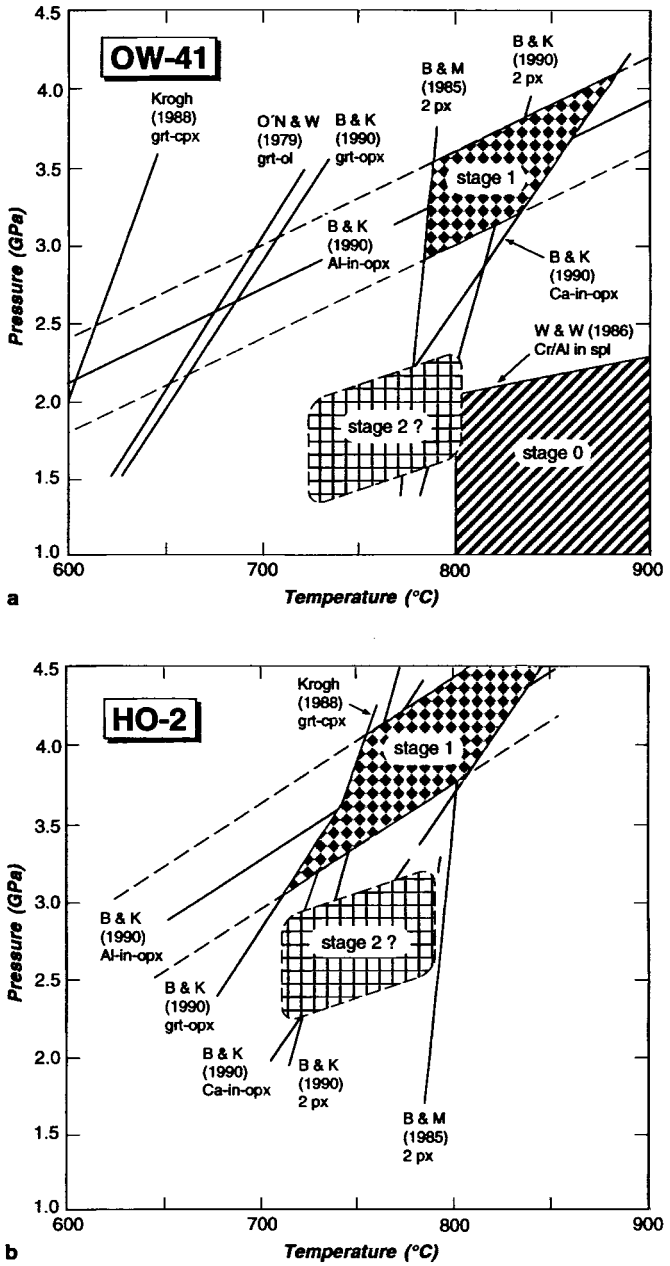

Fig. 6a, b Results of thermobarometric calculations for different evolutionary stages of garnet websterites. The stage 0 field in **a** is based on maximum pressures calculated from Webb and Wood (1986) and extends towards higher temperatures up to the peridotite solidus. *P-T* conditions for stage 1 are derived from graphical best fits of the thermometric and barometric results presented in Table 3 and in the section on thermobarometry. The formulations used are indicated on the figures. The *P-T* field for stage 2 is only weakly defined by strongly scattering pressures and temperatures obtained from stage 2 assemblages with the same thermobarometric formulations as those used for stage 1 (see section on thermobarometry and Table 3)

except for some scarce occurrences in the immediate vicinity of eclogites (Wimmenauer and Stenger 1989). Ultramafic *HP* rocks and eclogites could thus be confined to comparatively thin layers or nappes of lithospheric mantle material that were either intensively folded into a homogeneous *HT* basement or tectonically stacked between different crustal segments which are yet to be recognized. Concluding, it must be stressed that further petrological, geochronological, and structural data on the CSGC are needed to allow for definite conclusions on this problem.

Comparison with other Moldanubian peridotite and pyroxenite occurrences

Comparison of petrological data on different peridotites and pyroxenites within the Moldanubian zone is hampered by (1) the lacking correlation of geological units from different parts of the Moldanubian; (2) the lack of detailed petrographic descriptions and comprehensive mineral data for numerous occurrences; (3) the fact that different geothermometers and geobarometers have been applied to the various occurrences. Therefore, any comparison can only constrain similarities or differences in a very general way.

In general, the investigated ultramafic *HP* rocks of the Schwarzwald have lower equilibration temperatures compared to other Moldanubian garnet peridotite and pyroxenite occurrences. Ultramafic *HP* rocks comparable to the magnesian garnet-spinel peridotites from the Schwarzwald in terms of their *P-T* evolution are the garnet-spinel peridotites near Artiges in the French Massif Central (Bonnot and Piboule 1980) for which equilibration conditions of $974 \pm 88°$ C and 1.63 ± 0.34 GPa have been calculated (Medaris and Carswell 1990).

Comparatively ferriferous garnet peridotites or pyroxenites similar to the garnet websterites investigated here have only rarely been mentioned from other parts of the Moldanubian zone (Bonnet and Piboule 1980) and no *P-T* calculations are available. The *P-T* conditions of equilibration for many magnesian garnet peridotite occurrences within the Variscan belt have been calculated by Medaris and Carswell (1990). Their results show significantly higher temperatures (910–1264° C) at pressures between 2.2 and 5.1 GPa. Rocks that have experienced a *P-T* evolution similar to that of the Schwarzwald websterites (early *HT* stage within the spinel stability field followed by re-equilibration within the garnet stability field) have been described from western Moravia (Medaris et al. 1990) but yield higher temperature and lower pressure estimates than those from the Schwarzwald. In general, equilibration conditions of the Schwarzwald garnet pyroxenites are more similar to those of the Caledonian occurrences in Norway (Medaris 1984; Carswell 1986).

Conclusions

Mineralogical and microstructural studies as well as thermobarometric calculations on four garnet-bearing

ultramafic *HP* rocks, intercalated in *HT* gneisses and migmatites of the CSGC (Schwarzwald), lead to the following conclusions:

1. Garnet-(olivine) websterites experienced a *HT*-*HP* stage followed by equilibration at 740–850° C/ 3.2–4.3 GPa and subsequent recrystallization at lower pressures.
2. Magnesian garnet-spinel peridotites lack a *HT* stage and have equilibrated at significantly lower pressures of 1.4 to 1.8 GPa and slightly lower temperatures (670–740° C), corresponding to the equilibration conditions of the Schwarzwald eclogites.
3. From these results, contrasting *P-T* evolutions during Variscan convergence emerge for these two groups of rocks.
4. The garnet-bearing ultramafic *HP* rocks of the Schwarzwald presented here have lower equilibration temperatures compared to other Variscan garnet peridotites and pyroxenites.

Appendix

Sample locations

The investigated samples have the following locations of the Topographische Karte der Bundesrepublik Deutschland, 1: 25,000:

OW-41: sheet 7615 Wolfach, r 344413, h 535198; HO-2: sheet 7715 Hornberg, r 343885, h 535057; HH-10: sheet 8114 Feldberg, r 342534, h 529937; KA-1: sheet 8013 Freiburg r 341758, h 531282.

Analytical techniques

Mineral analyses were performed using a Camebax SX 50 microprobe equipped with 4 wavelength-dispersive spectrometers. Operating parameters were 20 s counting time (15 s for Na, K), 10 nA beam current, and 15 kV accelerating voltage. PAP correction was applied to the data. Natural and synthetic oxide and silicate standards were used for calibration.

Acknowledgements The authors would like to thank Hans-Peter Meyer for help with the microprobe work and with formula and *P-T* calculation programs. B.W. Evans and M. Raith are thanked for careful and constructive reviews.

References

Anderson MW, Barker AJ, Benett DJ, Dallmeyer RD (1992) A tectonic model for Scandian terrane accretion in the northern Scandinavian Caledonides. J Geol Soc London 149:727–741

Beard BL, Medaris LG Jr, Johnson CM, Brueckner HK, Misar Z (1992) Petrogenesis of Variscan high-temperature Group A eclogites from the Moldanubian zone of the Bohemian Massif, Czechoslovakia. Contrib Mineral Petrol 111:468–483

Bertrand P, Mercier J-CC (1985) The mutual solubility of coexisting ortho- and clinopyroxene: towards an absolute geothermometer for the natural system? Earth Planet Sci Lett 76:109–122

Bonnot H, Piboule M (1980) Mise en évidence d'une dualité d'origine des ultrabasites à grenat du Limousin et recherche de la signification des péridotites d'origine mantellique dans le Massif Central francais. C R Acad Sci Paris 291 Ser D:129–132

Brey GP, Köhler T (1990) Geothermobarometry in four-phase lherzolites. II. New thermobarometers, and practical assessment of existing thermobarometers. J Petrol 31:1353–1378

Brey GP, Köhler T, Nickel G (1990) Geothermobarometry in four-phase lherzolites. I. Experimental results from 10 to 60 kbar. J Petrol 31:1313–1352

Brueckner HK, Medaris LG Jr, Bakun-Czubarov N (1991) Nd and Sr age and isotope patterns from Variscan eclogites of the eastern Bohemian Massif. Neues Jahrb Mineral Abh 163:169–196

Canil D (1991) Experimental evidence for the exsolution of cratonic peridotite from high-temperature harzburgite. Earth Planet Sci Lett 106:64–72

Canil D (1992) Orthopyroxene stability along the peridotite solidus and the origin of cratonic lithosphere beneath southern Africa. Earth Planet Sci Lett 111:83–95

Carswell DA (1973) Garnet pyroxenite lens within Ugelvik layered garnet peridotite. Earth Planet Sci Lett 20:347–352

Carswell DA (1986) The metamorphic evolution of Mg-Cr type Norwegian garnet peridotites. Lithos 19:279–297

Carswell DA, Harley SL (1990) Mineral barometry and thermometry. In: Carswell DA (ed) Eclogite facies rocks. Blackie, Glasgow, pp 83–110

Carswell DA, Jamtveit B (1990) Variscan Sm-Nd ages for the high-pressure metamorphism in the Moldanubian Zone of the Bohemian Massif, Lower Austria. Neues Jahrb Mineral Abh 162:69–78

Carswell DA, Harvey MA, Al-Samman A (1983) The petrogenesis of contrasting Fe-Ti and Mg-Cr garnet peridotite types in the high-grade gneiss complex of western Norway. Bull Mineral 106:727–750

Chakraborty S, Ganguly J (1992) Cation diffusion in aluminosilicate garnets: experimental determination in spessartine-almandine diffusion couples, evaluation of effective binary diffusion coeffi-cients, and applications. Contrib Mineral Petrol 111:74–86

Dawson JB, Smith JV, Hervig FRS, Hervig RL (1980) Heterogeneity in upper-mantle lherzolites and harzburgites. Philos Trans R Soc London A297:323–331

Echtler HP, Chauvet A (1991/92) Carboniferous convergence and subsequent crustal extension in the southern Schwarzwald (SW Germany). Geodinamica Acta 5:37–49

Eisbacher GH, Lüschen E, Wickert F (1989) Thrusting and extension in the Hercynian Schwarzwald and Vosges, Central Europe. Tectonics 8:2–21

Elphick SC, Ganguly J, Loomis TP (1985) Experimental determination of cation diffusivities in aluminosilicate garnets. Contrib Mineral Petrol 90:36–44

Ernst WG (1978) Petrochemical study of lherzolitic rocks from the Western Alps. J Petrol 19:341–392

Evans BW, Trommsdorff V (1978) Petrogenesis of garnet lherzolite, Cima di Gagnone, Lepontine Alps. Earth Planet Sci Lett 40:333–348

Finnerty AA, Boyd FR (1987) Thermobarometry for garnet-peridotite xenoliths: a basis from upper mantle stratigraphy. In: Nixon PH (edn) Mantle xenoliths. Wiley and Sons, New York, pp 381–402

Frey FA (1980) The origin of pyroxenites and garnet pyroxenites from Salt Lake Crater, Oahu, Hawaii: trace element evidence. Am J Sci 280-A:427–449

Gasparik T (1987) Orthopyroxene thermometry in simple and complex systems. Contrib Mineral Petrol 96:357–370

Green DH, Ringwood AE (1967) The stability fields of aluminous pyroxene peridotite and garnet peridotite and their relevance in upper mantle structure. Earth Planet Sci Lett 3:151–160

Harley SL, Carswell DA (1990) Experimental studies on the stability of eclogite facies mineral parageneses. In: Carswell DA (ed) Eclogite facies rocks. Blackie, Glasgow, pp 53–82

Herzberg C, Gasparik T, Sawamoto H (1990) Origin of mantle peridotite: constraints from melting experiments to 16.5 GPa. J Geophys Res 95:15779–15803

Irving AJ (1980) Petrology and geochemistry of composite ultramafic xenoliths in alkalic basalts and implications for magmatic processes within the mantle. Am J Sci 280-A: 389–426

Jamtveit B (1987a) Metamorphic evolution of the Eiksunddal eclogite complex, western Norway, and some tectonic implications. Contrib Mineral Petrol 95: 82–99

Jamtveit B (1987b) Magmatic and metamorphic controls on chemical variations within the Eiksunddal eclogite complex, Sunnmøre, western Norway. Lithos 20: 369–389

Jenkins DM (1981) Experimental phase relations of hydrous peridotites modelled in the system H_2O-CaO-MgO-Al_2O_3-SiO_2. Contrib Mineral Petrol 77: 166–176

Jenkins DM (1983) Stability and composition relations of calcic amphiboles in ultramafic rocks. Contrib Mineral Petrol 83: 375–384

Jenkins DM, Newton RC (1979) Experimental determination of the spinel peridotite to garnet peridotite inversion at 900° C and at 1100° C in the system CaO-MgO-Al_2O_3-SiO_2, and at 900° C with natural garnet and olivine. Contrib Mineral Petrol 68: 407–419

Kalt A, Grauert B, Baumann A (1994a) Rb-Sr and U-Pb studies on migmatites from the Schwarzwald (F.R.G.) : constraints on isotopic resetting during high-temperature metamorphism. J Metamorphic Geol 12: 667–680

Kalt A, Hanel M, Schleicher H, Kramm U (1994b) Petrology and geochronology of eclogites from the Variscan Schwarzwald (F.R.G.). Contrib Mineral Petrol 115: 287–302

Krogh EJ (1988) The garnet-clinopyroxene Fe-Mg geothermometer – a reinterpretation of existing experimental data. Contrib Mineral Petrol 99: 44–48

Kushiro I, Shimizu N, Nakamura Y, Akimoto S (1972) Compositions of coexisting liquid and solid phases formed upon melting of natural garnet and spinel lherzolites at high pressures: a preliminary report. Earth Planet Sci Lett 14: 19–25

Loubet M, Allègre CJ (1982) Trace elements on orogenic lherzolites reveal the complex history of the upper mantle. Nature 298: 809–814

Medaris LG (1984) A geothermobarometric investigation of the garnet-peridotites in the western Gneiss Region of Norway. Contrib Mineral Petrol 87: 72–86

Medaris LG, Carswell DA (1990) Petrogenesis of Mg-Cr garnet peridotites in European metamorphic belts. In: Carswell DA (ed) Eclogite facies rocks. Blackie, Glasgow London, pp 260–290

Medaris LG, Wang HF, Mísar Z, Jelínek E (1990) Thermobarometry, diffusion modelling and cooling rates of crustal garnet peridotites: two examples from the Moldanubian zone of the Bohemian Massif. Lithos 25: 189–202

Obata M (1980) The Ronda Peridotite: garnet-, spinel-, and plagioclase-lherzolite facies and the *P-T* trajectories of a high-temperature mantle intrusion. J Petrol 21: 533–572

Obata M, Morten L (1987) Transformation of spinel lherzolite to garnet lherzolite in the ultramafic lenses of the Austridic Crystalline Complex, Northern Italy. J Petrol 28: 599–623

Obata M, Thompson AB (1981) Amphibole and chlorite in mafic and ultramafic rocks in the lower crust and the upper mantle. Contrib Mineral Petrol 77: 74–81

O'Neill HStC, Wood BJ (1979) An experimental study of Fe-Mg partitioning between garnet and olivine and its calibration as a geothermometer. Contrib Mineral Petrol 70: 59–70

Rey P, Burg J-P, Caron J-M (1991) Tectonique extensive ductile et plutonisme viséo-namurien dans les Vosges. C R Acad Sci Paris 312 Ser II: 1609–1616

Searle MP, Waters DJ, Rex DC, Wilson RN (1992) Pressure-temperature and time constraints on Himalayan metamorphism from eastern Kashmir and western Zanskar. J Geol Soc London 149: 753–773

Stenger R, Baatz K, Klein H, Wimmernauer W (1989) Metamorphic evolution of the pre-Hercynian basement of the Schwarzwald (Federal Republic of Germany). Tectonophysics 157: 117–121

Takahashi E (1990) Speculations on the Archean mantle: missing link between komatiite and depleted garnet peridotite. J Geophys Res 95: 15941–15954

Thompson AB, England P (1984) Pressure-temperature-time paths of regional metamorphism. II. Their inference and interpretation using mineral assemblages in metamorphic rocks. J Petrol 25: 929–955

Todt W (1976) Zirkon U/Pb-Alter des Malsburg-Granits vom Südschwarzwald. Neues Jahrb Mineral Monatsh 12: 532–544

Webb SAC, Wood BJ (1986) Spinel-pyroxene-garnet relationships and their dependence on Cr/Al ratio. Contrib Mineral Petrol 92: 471–480

Wendt I, Lenz H, Höhndorf A (1974) Das Alter des Bärhalde-Granites (Schwarzwald) und der Uranlagerstätte Menzenschwand. Geol Jahrb E2: 131–143

Wickert F, Altherr R, Deutsch M (1990) Polyphase Variscan tectonics and metamorphism along a segment of the Saxothuringian–Moldanubian boundary: the Baden-Baden Zone, northern Schwarzwald (F.R.G.). Geol Rundsch 79: 627–647

Wimmenauer W, Schreiner A (1981) Geologische Karte Baden-Württemberg 1: 25,000, Erläuterungen Blatt 8114 Feldberg, Stuttgart

Wimmenauer W, Stenger R (1989) Acid and intermediate *HP* metamorphic rocks in the Schwarzwald (Federal Republic of Germany). Tectonophysics 157: 109–116